



**HAL**  
open science

## **Astrocyte aquaporin mediates a tonic water efflux maintaining brain homeostasis**

Cuong Pham, Yuji Komaki, Anna Deàs-Just, Benjamin Le Gac, Christine Mouffle, Clara Franco, Vincent Vialou, Tomokazu Tsurugizawa, Bruno Cauli, Dongdong Li

► **To cite this version:**

Cuong Pham, Yuji Komaki, Anna Deàs-Just, Benjamin Le Gac, Christine Mouffle, et al.. Astrocyte aquaporin mediates a tonic water efflux maintaining brain homeostasis. *eLife*, 2023, 13, pp.RP95873. 10.7554/eLife.95873 . hal-04235174

**HAL Id: hal-04235174**

**<https://hal.science/hal-04235174v1>**

Submitted on 10 Oct 2023

**HAL** is a multi-disciplinary open access archive for the deposit and dissemination of scientific research documents, whether they are published or not. The documents may come from teaching and research institutions in France or abroad, or from public or private research centers.

L'archive ouverte pluridisciplinaire **HAL**, est destinée au dépôt et à la diffusion de documents scientifiques de niveau recherche, publiés ou non, émanant des établissements d'enseignement et de recherche français ou étrangers, des laboratoires publics ou privés.



Distributed under a Creative Commons Attribution 4.0 International License

*Pham et al., 2023*

1 **Astrocyte aquaporin mediates a tonic water efflux maintaining**  
2 **brain homeostasis**

3  
4 Cuong Pham<sup>1</sup>, Yuji Komaki<sup>2</sup>, Anna Deàs-Just<sup>1</sup>, Benjamin Le Gac<sup>1</sup>, Christine Mouffle<sup>1</sup>, Clara  
5 Franco<sup>1</sup>, Vincent Vialou<sup>1</sup>, Tomokazu Tsurugizawa<sup>3,4,#</sup>, Bruno Cauli<sup>1,#</sup>, Dongdong Li<sup>1,#</sup>

6  
7 <sup>1</sup>Sorbonne Université, Institute of Biology Paris Seine, Neuroscience Paris Seine, CNRS  
8 UMR8246, INSERM U1130, Paris 75005, France

9 <sup>2</sup>Central Institute for Experimental Animals, Kawasaki, Japan

10 <sup>3</sup>Human Informatics and Interaction Research Institute, National Institute of Advanced Industrial  
11 Science and Technology (AIST), Tsukuba, Japan

12 <sup>4</sup>Faculty of Engineering, University of Tsukuba, Tsukuba, Japan

13 #Correspondence: [tsurugizawa@hotmail.com](mailto:tsurugizawa@hotmail.com), [bruno.cauli@upmc.fr](mailto:bruno.cauli@upmc.fr), [dongdong.li@inserm.fr](mailto:dongdong.li@inserm.fr)

14

15 **Keywords:** imaging, swelling, diffusion

16

17

Pham et al., 2023

## 1 **ABSTRACT**

2 Brain water homeostasis provides not only physical protection, but also determines the diffusion  
3 of chemical molecules key for information processing and metabolic stability. As a major type of  
4 glial cell in the brain parenchyma, astrocytes are the dominant cell type expressing aquaporin  
5 water channels. However, how astrocyte aquaporin contributes to brain water homeostasis  
6 remains to be understood. We report here that astrocyte aquaporin 4 (AQP4) mediates a tonic  
7 water efflux in basal conditions. Acute inhibition of astrocyte AQP4 leads to intracellular water  
8 accumulation as optically resolved by fluorescence-translated imaging in acute brain slices, and  
9 *in vivo* by fiber photometry in moving mice. We then show that the tonic aquaporin water efflux  
10 maintains astrocyte volume equilibrium, astrocyte and neuron  $\text{Ca}^{2+}$  signaling, and extracellular  
11 space remodeling during optogenetically induced cortical spreading depression. Using diffusion-  
12 weighted magnetic resonance imaging (DW-MRI), we observed that *in vivo* inhibition of AQP4  
13 water efflux heterogeneously disturbs brain water homeostasis in a region-dependent manner.  
14 Our data suggest that astrocyte aquaporin, though bidirectional in nature, mediates a tonic water  
15 outflow to sustain cellular and environmental equilibrium in brain parenchyma.

16

*Pham et al., 2023*

## 1 **Significance statement**

2 Our brain is immersed, thus protected, in a water environment. It ensures intra- and extracellular  
3 molecular diffusion, which is vital for brain function and health. Brain water homeostasis is  
4 maintained by dynamic water transport between different cell types. Astrocytes are a main type  
5 of glial cell widely distributed in brain parenchyma, and are also the primary cell type expressing  
6 the bidirectional aquaporin water channel. Here we show that in basal conditions, aquaporin  
7 channel mediates a tonic water efflux from astrocytes. This mechanism maintains astrocyte  
8 volume stability, activity-gated brain parenchyma remodeling and brain water homeostasis. Our  
9 finding sheds light on how astrocytes regulate water states in the brain, and will help to  
10 understand brain homeostasis in specific life context.

11

12

13

Pham et al., 2023

1 \body

## 2 **Introduction**

3 Every aspect of brain function relies on the delicately maintained water environment. It supports  
4 brain structural stability and molecular diffusion, laying the ground for information processing,  
5 metabolite shuttling and adaptation to living environments (1). Water is the fundamental  
6 constituent of the cerebrospinal fluid infiltrating into the central nervous system and the  
7 interstitial fluid distributed in brain parenchyma (2, 3). Brain fluid transport is suggested to  
8 support the diffusion of energetic fuels like glucose and lactate to warrant the metabolic  
9 circumstances in the parenchyma, and is also implicated in the clearance of waste molecules  
10 from the brain as described in the glymphatic system (4, 5). In addition, brain water diffusion is  
11 the basis for diffusion-weighted magnetic resonance imaging (DW-MRI) for structural and  
12 functional neuroimaging (6), and for clinical diagnostics widely applied for neurological diseases  
13 such as ischemia, brain tumor and edema (7, 8).

14 Water equilibrium in the brain is maintained by dynamic transport between different cell  
15 entities. Aquaporin is a family of transmembrane channels facilitating bidirectional water flow,  
16 with aquaporin 4 (AQP4) being the main subtype expressed in the central nervous system. In the  
17 brain, AQP4 is predominantly expressed in astrocytes (9, 10) that are a major type of glial cells  
18 distributed throughout the parenchyma (11). This feature renders astrocytes well equipped to  
19 balance osmotic oscillations imposed by the transmembrane transport of ions, metabolites, and  
20 signaling molecules, all mediated by water. However, thus far, how astrocyte aquaporin  
21 contributes to brain water homeostasis remains elusive.

22 Here, combining *in vivo* chemical targeting and optical water transport imaging, we  
23 report that AQP4 sustains a tonic water efflux from astrocytes. This mechanism was found to be

Pham et al., 2023

1 critical in maintaining astrocyte volume and signaling stability, as well as the extracellular space  
2 remodeling in mouse cortex. Using DW-MRI, we observed that acute inhibition of astrocyte  
3 water efflux *in vivo* causes heterogeneous alterations in brain water diffusion. Our finding  
4 suggests that aquaporin acts as an important water export route in astrocytes, to counterbalance  
5 excessive water accumulation in the cytoplasm. This mechanism plays a necessary role in  
6 maintaining water equilibrium in astrocytes, thereby the water homeostasis in the brain.

7

8

## 9 **Results**

### 10 **Astrocyte aquaporin mediates a tonic water efflux**

11 To follow *in situ* astrocyte water transport, we performed fluorescence intensity-translated (FIT)  
12 imaging. To this end, mouse brain astrocytes were chemically labeled *in vivo* with a highly  
13 water-diffusible and astrocyte-specific red fluorescent dye, sulforhodamine B (SRB) (Fig. 1A)  
14 (12, 13). About one hour after its intraperitoneal injection, astrocytic SRB labeling was widely  
15 distributed in the mouse cortex, as seen in living acute brain slices (Fig. 1A) and validated by  
16 colocalization with EGFP-identified astrocytes in slices taken from GFAP-EGFP transgenic mice  
17 (Fig. 1A). Net water transport across the astrocyte membrane alters cytoplasmic SRB  
18 concentration and cellular volume, which can thus be followed by changes in fluorescence  
19 intensity when imaged in a fixed field of view. To validate the FIT imaging of astrocyte water  
20 transport, we employed wide-field fluorescence microscopy for single-plane time-lapse imaging  
21 in acute brain slices in the primary somatosensory (S1) cortex. This approach allowed us to  
22 collect fluorescence from both the focal plane and along the axial extensions, thereby imprinting  
23 volumetric fluorescence into the single image plane. Indeed, water influx induced by the

*Pham et al., 2023*

1 hypoosmotic solution caused decreases in astrocyte SRB fluorescence in a time-dependent  
2 manner which also reflected cell swelling (Fig. 1B); whereas water export and astrocyte  
3 shrinking upon hyperosmotic manipulation increased astrocyte fluorescence (Fig. 1B). Hence,  
4 FIT imaging enables real-time recording of astrocyte transmembrane water transport and volume  
5 dynamics.

6 In basal conditions, flat fluorescence time course was recorded suggesting equilibrated  
7 water transport across the astrocyte membrane (Fig. 1B) and volume homeostasis in the brain  
8 parenchyma. To inspect a tonic role of aquaporin in astrocyte water transport, we sought to  
9 acutely block the astrocyte aquaporin channel, aquaporin 4 (AQP4). We used the synthetic  
10 compound 2-(nicotinamido)-1,3,4-thiadiazole (TGN-020) that is derived from the condensation  
11 of nicotinamide and thiadiazole derivatives (14, 15), whose specificity for AQP4 has been  
12 validated *in vitro* by ion channel heterologous expression system (16) and *in vivo* using the  
13 knockout mouse model (17, 18). This approach guaranteed the functional pinpointing of  
14 astrocyte aquaporin under physiological conditions, while avoiding the chronic compensations  
15 caused by genetic tools and mouse models that have been reported to alter brain water content,  
16 volume and extracellular space potentially confounding the functional readouts (19-23).

17 AQP4 is a bidirectional channel facilitating passive water transport along the osmotic  
18 gradient (9). As an osmotic equilibrium is maintained in the brain parenchyma in basal state,  
19 there might not be net water transport across AQP4. However, we observed in cortical slices that  
20 acute inhibition of astrocyte AQP4 by TGN-020 gradually induced intracellular water  
21 accumulation, evidenced by a decrease in SRB fluorescence intensity as a result of cytosolic  
22 dilution (Fig. 1C). This observation suggests that astrocyte aquaporin mediates a tonic water  
23 efflux; its blocking causes intracellular water accumulation and swelling (Fig. 1C, right). To

Pham et al., 2023

1 corroborate this observation *in vivo*, we performed fiber photometry recording in moving mice  
2 (Fig. 1D). An optical fiber was implanted into the mouse S1 cortex to follow fluorescence  
3 signals of local astrocyte population post the intraperitoneal injection of SRB (Fig. 1D, left).  
4 After about one hour, when astrocytes were well labeled, either saline or TGN-020 was injected  
5 intraperitoneally. While no significant effect was observed with the saline control, TGN-020  
6 induced a decrease in astrocyte SRB fluorescence and a reduction in its oscillation range (Fig.  
7 1D, right), mirroring an intracellular dilution of fluorescent molecules. This observation  
8 confirms that acute inhibition of astrocyte aquaporin leads to intracellular water accumulation  
9 thereby cell swelling.

10

### 11 **Aquaporin inhibition perturbs astrocyte and neuron signaling**

12 Astrocyte volume equilibrium not only determines brain architectural stability, but also  
13 associates with dynamic cellular signals. Indeed, astrocyte swelling has been shown to alter  
14 intracellular  $\text{Ca}^{2+}$  signaling (24, 25). We then performed  $\text{Ca}^{2+}$  imaging to confirm that acute  
15 aquaporin inhibition induces astrocyte swelling and thus  $\text{Ca}^{2+}$  oscillation. The genetically  
16 encoded  $\text{Ca}^{2+}$  sensor GCaMP6 was selectively expressed in astrocytes by crossing the Glast-  
17  $\text{Cre}^{\text{ERT2}}$  and GCaMP6<sup>floxP</sup> mouse line (13, 26). Because astrocyte  $\text{Ca}^{2+}$  signals often occur in  
18 local domains, we adapted a light sheet microscope (13) for wide-field optical sectioning so as to  
19 image them with high signal-to-noise ratio (SI Appendix, Fig. S1). We first confirmed that water  
20 accumulation induced by hypotonic solution, therefore swelling, in astrocytes alters the  
21 intracellular  $\text{Ca}^{2+}$  signal (Fig. 2A). Then we followed astrocyte  $\text{Ca}^{2+}$  in isotonic control condition  
22 while only blocking astrocyte AQP4 with TGN-020.  $\text{Ca}^{2+}$  signaling was indeed altered upon  
23 acute inhibition of aquaporin (Fig. 2B), reflecting that restriction of tonic water efflux from



*Pham et al., 2023*

1 aquaporin leads to intracellular water accumulation, astrocyte swelling and modification of  $\text{Ca}^{2+}$   
2 oscillation. In addition, astrocyte swelling has been reported to induce the release of neuroactive  
3 molecules such as glutamate thereby influencing nearby neuron activity (27, 28). Hence,  
4 disrupting AQP4 tonic water outflow would not only cause astrocyte swelling but also influence  
5 the activity of neighboring neurons. To validate it, we imaged  $\text{Ca}^{2+}$  signals as a surrogate for  
6 neuronal activity in cortical somatostatin (SST) interneurons which exhibit the highest  
7 excitability (29) and express both ionotropic and metabotropic glutamate receptors (30), making  
8 them ideal to sense astrocyte-released signaling molecules. We expressed GCaMP6 in SST  
9 interneurons by crossing homozygous SST-Cre (31) and homozygous GCaMP6<sup>floxP</sup> mice. As  
10 expected, TGN-020 inhibition of astrocyte AQP4 led to a global  $\text{Ca}^{2+}$  elevation in SST  
11 interneuron populations (Fig. 2C). These observations support that astrocyte aquaporin mediates  
12 a tonic water efflux, contributing to maintain both the volume and signaling homeostasis.

13

#### 14 **Aquaporin water efflux regulates astrocyte volume response**

15 We then examined the role of aquaporin water efflux in astrocyte volume response to osmotic  
16 environments. We followed the evoked water efflux and shrinking induced by hypertonic  
17 solution. As astrocyte AQP4 supports preferentially water efflux, its inhibition would attenuate  
18 hypertonicity-imposed water extrusion (Fig. 3A). Supporting this, application of TGN-020  
19 slowed down the hypertonicity-induced water efflux and shrinking, reflected by the longer time  
20 to peak in the SRB fluorescence time course as compared to control (Fig. 3B), though the delay  
21 in the initial onset was not significantly prolonged. The maximal increase in astrocyte SRB  
22 fluorescence was lower in the presence of TGN-020, suggesting that AQP4 blocking reduced the  
23 overall amount of water efflux (Fig. 3B).

*Pham et al., 2023*

1           We next evoked water influx, thereby astrocyte swelling, by hypotonic solution in the  
2 presence or absence of TGN-020 (**Fig. 3C**). In contrast to the effects on hypertonicity-evoked  
3 water efflux, AQP4 acute inhibition was observed to accelerate both the initial water  
4 accumulation and the swelling rate in astrocytes, reflected by their earlier onset in decrease of  
5 SRB fluorescence and the faster reaching to the plateau value relative to the control condition  
6 (**Fig. 3D**). This observation cross-validates the role of astrocyte aquaporin in supporting water  
7 efflux, whereby its blockade facilitates the evoked water accumulation (**Fig. 3C**). The maximum  
8 decrease in astrocyte SRB fluorescence was observed to be reduced with aquaporin inhibition  
9 (**Fig. 3D**). TGN-020 was present prior to hypotonic challenge, which would have slightly swelled  
10 astrocytes due to the blockade of tonic water efflux, thereby constraining the range of subsequent  
11 swelling.

12           Astrocytes are widely distributed throughout the brain parenchyma, orchestrating water  
13 transport and volume homeostasis (32). Water outflow via astrocyte AQP4 may play a role in the  
14 structural remodeling of parenchyma at the global level. We then induced general cell swelling  
15 by triggering cortical spreading depression (CSD) (33, 34). To be orthogonal to the  
16 pharmacological control of astrocyte aquaporin, the CSD depolarization wave was initiated by  
17 optogenetically stimulating ChR2-expressing glutamatergic cells in the cortical slices of Emx1-  
18 Cre/Ai32ChR2 mice (35, 36), termed Opto-CSD (37). As cell swelling increases the  
19 transmittance of infrared light, we imaged Opto-CSD by the intrinsic optical signal (IOS) derived  
20 from infrared illumination (34, 38). The IOS displayed transient increase across cortical layers  
21 during the Opto-CSD (**Fig. 4A-C**). The biphasic starting of IOS coincided with a sharp response  
22 in the extracellular potential indicating the CSD initiation (*SI Appendix, Fig. S2A*). IOS signal  
23 contains a first peak reflecting the rapid CSD response (**Fig. 4C, b**) followed by a prolonged

Pham et al., 2023

1 phase of general cellular swelling (Fig. 4C, c). By combining fluorescence imaging of SRB-  
2 labelled astrocytes, whose spectrum is separated from the IOS infrared signal, we observed that  
3 astrocytes swelling (i.e., decrease in SRB fluorescence) paralleled CSD swelling (SI Appendix,  
4 Fig. S3). Consistent with our observation on astrocyte volume response (Fig. 3D), when pre-  
5 incubating slices with TGN-020 to AQP4 tonic water outflow, the initiation of both the CSD and  
6 general swelling was accelerated while their maximum amplitude reduced (Fig. 4D-E; SI  
7 Appendix, Fig. S2B). Blocking action potentials with tetrodotoxin (TTX) only reduced the  
8 amplitude of the initial CSD response while the effect on general swelling is insignificant (Fig.  
9 4D-E). We further followed the swelling (i.e., water influx) of SRB-labeled astrocytes during  
10 Opto-CSD. In consistence with the result obtained from hypotonic challenge (Fig. 3D), the pre-  
11 presence of TGN-020 reduced the peak amplitude of astrocyte swelling (Fig. 4F). Notably,  
12 TGN-020 significantly inhibited astrocyte recovery from the swelling state (Fig. 4F), indicating  
13 that blocking AQP4 hinders the water efflux required for astrocyte volume maintenance.

14 Collectively, our data show that astrocyte AQP4 sustains a tonic water outflow regulating  
15 the cellular volume response and the general cell swelling of parenchyma.

16

### 17 **Tonic astrocyte water transport underlies brain homeostasis**

18 Water homeostasis sets the basis for molecular diffusion in the brain, which instructs  
19 neurotransmitter availability, ion recycling and metabolite trafficking. We then examined *in vivo*  
20 the role of astrocyte aquaporin outflow in brain water diffusion using DW-MRI (8). It uses the  
21 diffusion of water molecules to generate contrast that can be quantified by the apparent diffusion  
22 coefficient (ADC) in the nerve tissue (39, 40). We used a 7T MRI to image global brain water  
23 diffusion in lightly anesthetized mice with medetomidine, while acutely perturbing astrocyte

Pham et al., 2023

1 AQP4 outflow by TGN-020 via intraperitoneal injection. Brain water diffusion was mapped  
2 every 5 min before and after TGN or saline (as control) administration (Fig. 5A). Each  
3 acquisition sweep was performed with three b values (0, 250, 1800) that accounted for ADC, so  
4 to fit the exponential curve (Fig. 5B). Compared to the control saline, TGN-020 significantly  
5 increased basal water diffusion within multiple regions including the cortex, hippocampus and  
6 the striatum in a heterogeneous manner (Fig. 5C). The temporal features in water diffusion  
7 change appeared to be also different: an early elevation followed by a reversible tendency was  
8 observed for cortical areas, a rapid and long-lasting elevation for the striatum while a delayed  
9 and transient increase for the hippocampus (Fig. 5D). The *in vivo* neuroimaging results confirm  
10 that the tonic water efflux from astrocyte aquaporin contributes to maintain the homeostasis of  
11 brain water diffusion, and also suggest regional and temporal heterogeneities in brain water  
12 handling.

13

14

## 15 Discussion

16 Water equilibrium sets the basis for brain function, plasticity and dynamics. Astrocytes are the  
17 principal brain cell type expressing aquaporin water channels that are highly implicated in  
18 maintaining local environments (10). We show that albeit being a bidirectional channel, astrocyte  
19 aquaporin sustains a tonic water outflow in basal states to ensure the structural and functional  
20 stability, as well as brain water homeostasis.

21 The observation of a basal aquaporin water efflux implies there is constitutive water  
22 accumulation in brain astrocytes. As a ubiquitous vehicle for transporting ions, transmitters and  
23 metabolites, water enters astrocytes via a wide range of ion channels, transporters and

*Pham et al., 2023*

1 exchangers. For instance, they express  $\text{Na}^+/\text{K}^+$  and  $\text{Na}^+/\text{HCO}_3^-$  cotransporters to dynamically  
2 regulate intra- and extracellular ion homeostasis (21). Standing as a major glial cell type  
3 controlling the neuropil environment, astrocytes take up synaptically released  $\text{K}^+$  through  
4 inwardly rectified  $\text{K}^+$  channels and neurotransmitters (e.g., glutamate, GABA) via high-affinity  
5 transporters to safeguard synaptic transmission (41). The transmembrane molecular exchange  
6 may lead to continual water entry into astrocytes. Moreover, astrocytes juxtapose the cerebral  
7 vasculature, being a front relay station for brain metabolism. They express glucose transporter  
8 and lactate-permeable monocarboxylate transporters facilitating energy substrate uptake and  
9 transfer between blood vessels and neuron-glia networks (42). As water is produced during  
10 metabolic processes (43), astrocyte metabolism would also contribute to the constitutive water  
11 accumulation in the cytoplasm. An efficient efflux pathway appears necessary to counterbalance  
12 the excessive water buildup, thereby maintaining astrocyte and brain homeostasis. Our data  
13 suggest that astrocyte AQP4 fulfills such a role by supporting tonic water outflow (*SI Appendix,*  
14 *Fig. S4*). Our result echoes that in the principal cells of the kidney collecting duct, AQP4 is  
15 suggested to mainly mediate water exit to balance the AQP2-sustained water entry (44).

16 This study also provides mechanistic clues to understand AQP4-relevant pathologies in  
17 specific contexts. For instance, astrocyte water accumulation and swelling is a prominent cause  
18 of brain edema. The presence of AQP4 has been found to ameliorate perihematomal edema in  
19 intracerebral hemorrhage (45), which could be attributed to the contribution of AQP4 to  
20 astrocyte basal water extrusion. In neuromyelitis optica spectrum disorders, featured by  
21 circulating IgG autoantibody against AQP4, water transport ability is downregulated in  
22 astrocytes associated with swelling (46, 47). The inhibition of astrocyte AQP4 by autoantibody  
23 would reduce the tonic water efflux thereby causing progressive pathological swelling.

*Pham et al., 2023*

1           We observed that acutely blocking aquaporin caused basal water accumulation leading to  
2 swelling in astrocytes, and facilitated the evoked astrocyte swelling by hypoosmoticity and  
3 during cortical spreading depression. This recalls early observation by electron microscopy that  
4 knocking out the anchoring protein alpha-syntrophin to disperse AQP4 clustering induces an  
5 enlargement of astrocyte endfeet (48). It likely reflects astrocyte local swelling caused by the  
6 disruption of AQP4-mediated water efflux. Our observation also parallels the report that AQP4  
7 knock out facilitates astrocytes swelling induced by hypoosmotic solution (49). Nevertheless,  
8 genetic inactivation of AQP4 also reveals inhibitory effects on astrocyte swelling (24, 50, 51).  
9 Such discrepancy might be due to the variable compensations in brain water content and  
10 structure integrity during chronic genetic manipulations (19-22). Astrocyte aquaporin modulates  
11 brain water transport (21), though its role in the glymphatic system is under deliberation (52-55).  
12 Our data suggest that astrocyte aquaporin-mediated outflow helps to maintain local water  
13 environment in the brain parenchyma. Moreover, besides affecting water transport, targeting  
14 AQP4 also impacts astrocyte volume therefore the size of extracellular space. These two factors  
15 would need be considered when evaluating AQP4 involvement in brain fluid transport.

16           We show by DW-MRI that water transport by astrocyte aquaporin is critical for brain  
17 water homeostasis. When blocking AQP4 with TGN-020, therefore its basal water outflow, we  
18 observed spatially heterogeneous elevations of diverse temporal kinetics in brain water diffusion  
19 rate. Our current data are derived from 5 min apart acquisitions, providing information over the  
20 early phase of AQP4 inhibition therefore extending our early report (56). The regional  
21 heterogeneity likely reflects the various levels of AQP4 expression; its relative enrichment in the  
22 cerebral cortex (57) corresponds to the pronounced effect observed here by DW-MRI. An overall  
23 increase in brain water diffusion rate was observed when blocking AQP4 water efflux. This

*Pham et al., 2023*

1 treatment causes water accumulation inside astrocytes and their swelling, which reduces the  
2 extracellular space but increases the intracellular space. Water diffusion would be enhanced  
3 inside astrocytes and decreased in extracellular space, respectively. DW-MRI maps global water  
4 diffusion of both intra- and extracellular space. Likely, a net increase in brain water diffusion  
5 may reflect its intracellular increase exceeding the extracellular decrease. In addition, convective  
6 brain fluid flow has been suggested to be present in the perivascular space (52), a scenario  
7 extended by the glymphatic system to the extracellular space of the parenchyma (58). In this  
8 sense, squeezing of extracellular space might increase the rate of the water flow. The current  
9 MRI data yet lack sufficient spatial resolution to delineate the spatial compartmentalization of  
10 the brain fluid flow.

11 Our study sheds light on the mechanisms by which astrocyte aquaporin contributes to the  
12 water environment of brain parenchyma, and will help to understand the processes underlying  
13 the brain homeostasis and adaptation to life conditions.

14

15

## 16 **Materials and methods**

17 Experiments were undertaken in accordance with European Community guiding principles on  
18 the care and use of animals (86/609/CEE), and the rules of the host institute. For water transport  
19 and volume imaging, coronal slices comprising somatosensory cortex were acutely prepared  
20 from C57BL/6 mice of both sexes at ages of about 4-6 weeks, unless otherwise indicated. Light  
21 sheet and epifluorescence imaging were both performed on a wide-field upright microscope  
22 (Zeiss Axioskop 50, Germany). *In vivo* fiber photometry recording was performed using a  
23 Neurophotometrics system (FP3002). DW-MRI experiments were conducted on a Bruker 7T

*Pham et al., 2023*

- 1 scanner using a cryo-cooled mouse brain coil, mice being mildly anesthetized with
- 2 medetomidine (0.6 mg/kg/h, intravenous injection). Extended methods are provided in *SI*
- 3 *Appendix*.



Pham et al., 2023

## 1 **Acknowledgements and funding sources**

2 We thank the animal and imaging facilities of the IBPS (Sorbonne Université, Paris, France). We  
3 thank Nathalie Rouach for the GFAP-EGFP mice, Hervé Le Corronc and Thomas Panier for the  
4 discussion and the 3D printing of the light sheet chamber, respectively. This work was supported  
5 by the Agence Nationale de la Recherche (ANR-17-CE37-0010-03; ANR-20-CE14-0025-02),  
6 France Alzheimer individual fellowship (2021-2022), Japanese society for promotion of science  
7 (JSPS) 2022 summer grant, Grant-in-Aid for Challenging Research (Exploratory) in Japan (grant  
8 number 21K19464), the i-Bio initiative grant of Sorbonne Université.

9

## 10 **Supporting Information**

11 Extended methods and four supplementary figures (*SI Appendix, Fig. S1-S4*) are included.

12

## 13 **Competing interest**

14 The authors declare no competing financial interests.

15

## 16 **Data sharing plans**

17 The authors commit to share data, documentation, and code used in analysis.

18

19

1

2 **References:**

- 3 1. Kimelberg HK (2004) Water homeostasis in the brain: basic concepts. *Neuroscience* 129(4):851-  
4 860.
- 5 2. Brinker T, Stopa E, Morrison J, & Klinge P (2014) A new look at cerebrospinal fluid circulation.  
6 *Fluids Barriers CNS* 11:10.
- 7 3. Agnati LF, Marcoli M, Leo G, Maura G, & Guidolin D (2017) Homeostasis and the concept of  
8 'interstitial fluids hierarchy': Relevance of cerebrospinal fluid sodium concentrations and brain  
9 temperature control (Review). *Int J Mol Med* 39(3):487-497.
- 10 4. Louveau A, et al. (2017) Understanding the functions and relationships of the glymphatic system  
11 and meningeal lymphatics. *J Clin Invest* 127(9):3210-3219.
- 12 5. Abbott NJ, Pizzo ME, Preston JE, Janigro D, & Thorne RG (2018) The role of brain barriers in  
13 fluid movement in the CNS: is there a 'glymphatic' system? *Acta Neuropathol* 135(3):387-407.
- 14 6. Le Bihan D, Urayama S, Aso T, Hanakawa T, & Fukuyama H (2006) Direct and fast detection of  
15 neuronal activation in the human brain with diffusion MRI. *Proceedings of the National Academy  
16 of Sciences of the United States of America* 103(21):8263-8268.
- 17 7. Gaddamanugu S, et al. (2022) Clinical applications of diffusion-weighted sequence in brain  
18 imaging: beyond stroke. *Neuroradiology* 64(1):15-30.
- 19 8. Le Bihan D & Iima M (2015) Diffusion Magnetic Resonance Imaging: What Water Tells Us  
20 about Biological Tissues. *PLoS Biol* 13(7):e1002203.
- 21 9. Papadopoulos MC & Verkman AS (2013) Aquaporin water channels in the nervous system. *Nat  
22 Rev Neurosci* 14(4):265-277.
- 23 10. Xiao M, Hou J, Xu M, Li S, & Yang B (2023) Aquaporins in Nervous System. *Adv Exp Med Biol*  
24 1398:99-124.
- 25 11. Barres BA (2008) The mystery and magic of glia: a perspective on their roles in health and  
26 disease. *Neuron* 60(3):430-440.
- 27 12. Appaix F, et al. (2012) Specific in vivo staining of astrocytes in the whole brain after intravenous  
28 injection of sulforhodamine dyes. *PLoS One* 7(4):e35169.
- 29 13. Pham C, et al. (2020) Mapping astrocyte activity domains by light sheet imaging and spatio-  
30 temporal correlation screening. *Neuroimage* 220:117069.
- 31 14. Huber VJ, Tsujita M, & Nakada T (2009) Identification of aquaporin 4 inhibitors using in vitro  
32 and in silico methods. *Bioorg Med Chem* 17(1):411-417.
- 33 15. Burnett ME, Johnston HM, & Green KN (2015) Structural characterization of the aquaporin  
34 inhibitor 2-nicotinamido-1,3,4-thiadiazole. *Acta Crystallogr C Struct Chem* 71(Pt 12):1074-1079.
- 35 16. Toft-Bertelsen TL, et al. (2021) Clearance of activity-evoked K(+) transients and associated glia  
36 cell swelling occur independently of AQP4: A study with an isoform-selective AQP4 inhibitor.  
37 *Glia* 69(1):28-41.

- 1 17. Harrison IF, et al. (2020) Impaired glymphatic function and clearance of tau in an Alzheimer's  
2 disease model. *Brain* 143(8):2576-2593.
- 3 18. Igarashi H, Tsujita M, Suzuki Y, Kwee IL, & Nakada T (2013) Inhibition of aquaporin-4  
4 significantly increases regional cerebral blood flow. *Neuroreport* 24(6):324-328.
- 5 19. Haj-Yasein NN, et al. (2011) Glial-conditional deletion of aquaporin-4 (Aqp4) reduces blood-  
6 brain water uptake and confers barrier function on perivascular astrocyte endfeet. *Proceedings of*  
7 *the National Academy of Sciences of the United States of America* 108(43):17815-17820.
- 8 20. Binder DK, Papadopoulos MC, Haggie PM, & Verkman AS (2004) In vivo measurement of brain  
9 extracellular space diffusion by cortical surface photobleaching. *J Neurosci* 24(37):8049-8056.
- 10 21. MacAulay N (2021) Molecular mechanisms of brain water transport. *Nat Rev Neurosci*  
11 22(6):326-344.
- 12 22. Yao X, et al. (2015) Aquaporin-4 regulates the velocity and frequency of cortical spreading  
13 depression in mice. *Glia* 63(10):1860-1869.
- 14 23. Gomolka RS, et al. (2023) Loss of aquaporin-4 results in glymphatic system dysfunction via  
15 brain-wide interstitial fluid stagnation. *eLife* 12.
- 16 24. Benfenati V, et al. (2011) An aquaporin-4/transient receptor potential vanilloid 4 (AQP4/TRPV4)  
17 complex is essential for cell-volume control in astrocytes. *Proceedings of the National Academy*  
18 *of Sciences of the United States of America* 108(6):2563-2568.
- 19 25. Eilert-Olsen M, et al. (2019) Astroglial endfeet exhibit distinct Ca<sup>2+</sup> signals during  
20 hypoosmotic conditions. *Glia* 67(12):2399-2409.
- 21 26. Herrera Moro Chao D, et al. (2022) Hypothalamic astrocytes control systemic glucose  
22 metabolism and energy balance. *Cell metabolism* 34(10):1532-1547 e1536.
- 23 27. Fiacco TA, et al. (2007) Selective stimulation of astrocyte calcium in situ does not affect  
24 neuronal excitatory synaptic activity. *Neuron* 54(4):611-626.
- 25 28. Yang J, et al. (2019) Glutamate-Releasing SWELL1 Channel in Astrocytes Modulates Synaptic  
26 Transmission and Promotes Brain Damage in Stroke. *Neuron*.
- 27 29. Karagiannis A, et al. (2021) Lactate is an energy substrate for rodent cortical neurons and  
28 enhances their firing activity. *eLife* 10.
- 29 30. Cauli B, et al. (2000) Classification of fusiform neocortical interneurons based on unsupervised  
30 clustering. *Proceedings of the National Academy of Sciences of the United States of America*  
31 97(11):6144-6149.
- 32 31. Taniguchi H, et al. (2011) A resource of Cre driver lines for genetic targeting of GABAergic  
33 neurons in cerebral cortex. *Neuron* 71(6):995-1013.
- 34 32. Ochoa-de la Paz LD & Gullias-Canizo R (2022) Glia as a key factor in cell volume regulation  
35 processes of the central nervous system. *Front Cell Neurosci* 16:967496.
- 36 33. Zhao HH, et al. (2019) Time-resolved quantification of the dynamic extracellular space in the  
37 brain: study of cortical spreading depression. *Journal of neurophysiology* 121(5):1735-1747.
- 38 34. Holthoff K & Witte OW (1996) Intrinsic optical signals in rat neocortical slices measured with  
39 near-infrared dark-field microscopy reveal changes in extracellular space. *J Neurosci* 16(8):2740-  
40 2749.

- 1 35. Gorski JA, et al. (2002) Cortical excitatory neurons and glia, but not GABAergic neurons, are  
2 produced in the Emx1-expressing lineage. *J Neurosci* 22(15):6309-6314.
- 3 36. Madisen L, et al. (2012) A toolbox of Cre-dependent optogenetic transgenic mice for light-  
4 induced activation and silencing. *Nat Neurosci* 15(5):793-802.
- 5 37. Chung DY, et al. (2019) Determinants of Optogenetic Cortical Spreading Depolarizations. *Cereb*  
6 *Cortex* 29(3):1150-1161.
- 7 38. MacVicar BA & Hochman D (1991) Imaging of synaptically evoked intrinsic optical signals in  
8 hippocampal slices. *J Neurosci* 11(5):1458-1469.
- 9 39. Beaulieu C (2002) The basis of anisotropic water diffusion in the nervous system - a technical  
10 review. *NMR Biomed* 15(7-8):435-455.
- 11 40. Le Bihan D (2014) Diffusion MRI: what water tells us about the brain. *EMBO Mol Med* 6(5):569-  
12 573.
- 13 41. Dallerac G, Zapata J, & Rouach N (2018) Versatile control of synaptic circuits by astrocytes:  
14 where, when and how? *Nat Rev Neurosci* 19(12):729-743.
- 15 42. Cauli B, Dusart I, & Li D (2023) Lactate as a determinant of neuronal excitability,  
16 neuroenergetics and beyond. *Neurobiol Dis*:106207.
- 17 43. Bonvento G & Bolanos JP (2021) Astrocyte-neuron metabolic cooperation shapes brain activity.  
18 *Cell metabolism* 33(8):1546-1564.
- 19 44. Noda Y, Sohara E, Ohta E, & Sasaki S (2010) Aquaporins in kidney pathophysiology. *Nat Rev*  
20 *Nephrol* 6(3):168-178.
- 21 45. Jeon H, et al. (2021) Upregulation of AQP4 Improves Blood-Brain Barrier Integrity and  
22 Perihematomal Edema Following Intracerebral Hemorrhage. *Neurotherapeutics* 18(4):2692-2706.
- 23 46. Mireles-Ramirez MA, et al. (2022) Neuromyelitis optica spectrum disorder: pathophysiological  
24 approach. *Int J Neurosci*:1-13.
- 25 47. Lucchinetti CF, et al. (2014) The pathology of an autoimmune astrocytopathy: lessons learned  
26 from neuromyelitis optica. *Brain Pathol* 24(1):83-97.
- 27 48. Amiry-Moghaddam M, et al. (2003) An alpha-syntrophin-dependent pool of AQP4 in astroglial  
28 end-feet confers bidirectional water flow between blood and brain. *Proceedings of the National*  
29 *Academy of Sciences of the United States of America* 100(4):2106-2111.
- 30 49. Murphy TR, et al. (2017) Hippocampal and Cortical Pyramidal Neurons Swell in Parallel with  
31 Astrocytes during Acute Hypoosmolar Stress. *Front Cell Neurosci* 11:275.
- 32 50. Mola MG, et al. (2016) The speed of swelling kinetics modulates cell volume regulation and  
33 calcium signaling in astrocytes: A different point of view on the role of aquaporins. *Glia*  
34 64(1):139-154.
- 35 51. Woo J, et al. (2018) Astrocytic water channel aquaporin-4 modulates brain plasticity in both mice  
36 and humans: a potential gliogenetic mechanism underlying language-associated learning. *Mol*  
37 *Psychiatry* 23(4):1021-1030.
- 38 52. Smith AJ & Verkman AS (2019) CrossTalk opposing view: Going against the flow: interstitial  
39 solute transport in brain is diffusive and aquaporin-4 independent. *J Physiol* 597(17):4421-4424.

Pham *et al.*, 2023

- 1 53. Smith AJ, Yao X, Dix JA, Jin BJ, & Verkman AS (2017) Test of the 'glymphatic' hypothesis  
2 demonstrates diffusive and aquaporin-4-independent solute transport in rodent brain parenchyma.  
3 *eLife* 6.
- 4 54. Mestre H, *et al.* (2018) Aquaporin-4-dependent glymphatic solute transport in the rodent brain.  
5 *eLife* 7.
- 6 55. Rasmussen MK, Mestre H, & Nedergaard M (2022) Fluid transport in the brain. *Physiol Rev*  
7 102(2):1025-1151.
- 8 56. Debacker C, Djemai B, Ciobanu L, Tsurugizawa T, & Le Bihan D (2020) Diffusion MRI reveals  
9 in vivo and non-invasively changes in astrocyte function induced by an aquaporin-4 inhibitor.  
10 *PLoS One* 15(5):e0229702.
- 11 57. Clarke LE, *et al.* (2018) Normal aging induces A1-like astrocyte reactivity. *Proceedings of the*  
12 *National Academy of Sciences of the United States of America* 115(8):E1896-E1905.
- 13 58. Mestre H, *et al.* (2018) Flow of cerebrospinal fluid is driven by arterial pulsations and is reduced  
14 in hypertension. *Nature communications* 9(1):4878.

15

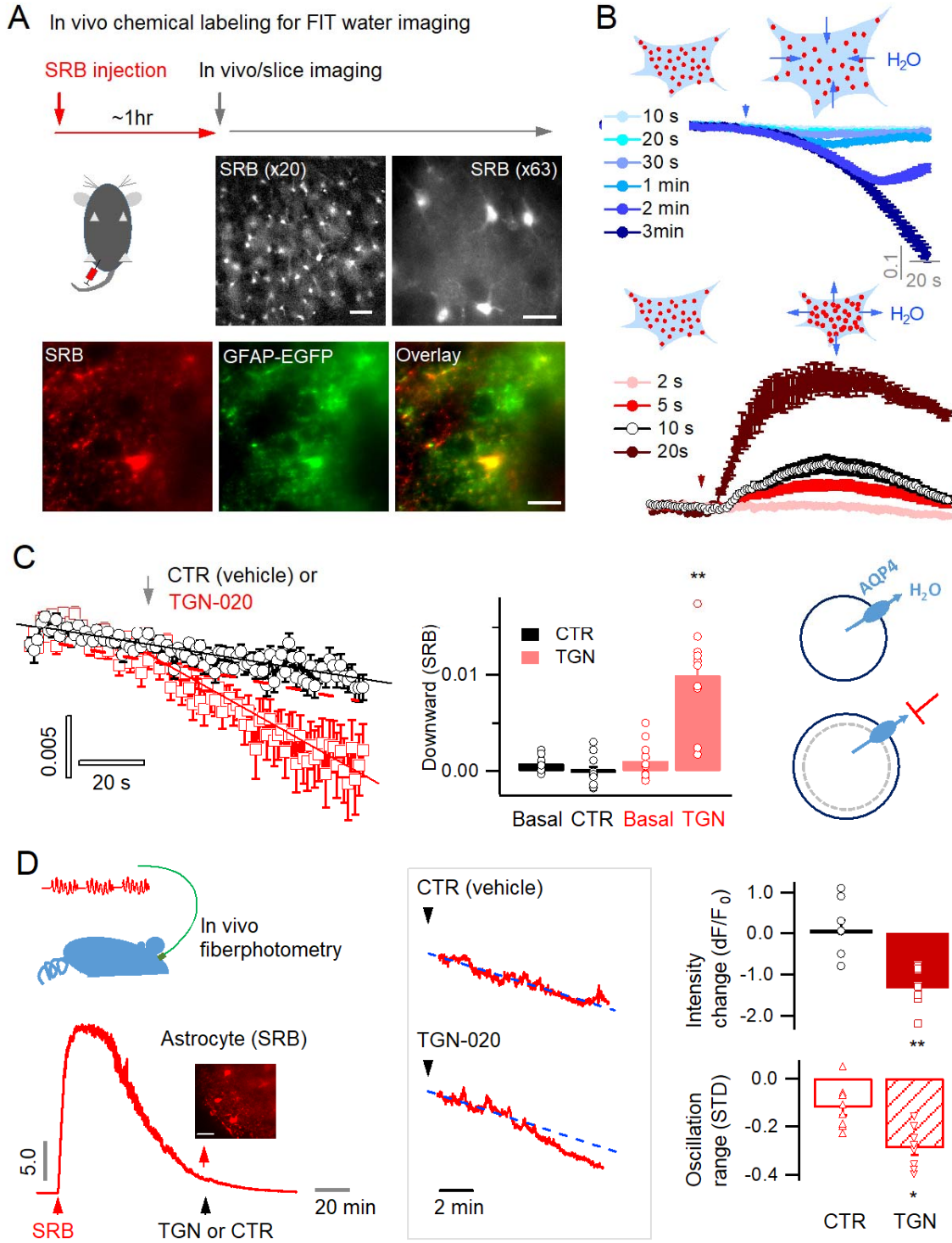


**FIGURE 1**

**Fig. 1.** Astrocyte aquaporin mediates a tonic water efflux. (A) *In vivo* chemical labelling of astrocytes. Sulforhodamine B (SRB, 10 mg/ml) was intraperitoneally injected in awake mice (10  $\mu$ l/g). Monochrome images show representative astrocyte labeling in living acute brain slices from cortex under low ( $\times 20$ ; scale bar, 50  $\mu$ m) and high magnification ( $\times 63$ ; scale bar, 20  $\mu$ m) by epifluorescence. *Below*, SRB labeling was confirmed to be astrocyte-specific in acute brain slices of the astrocyte reporter line GFAP-EGFP, where light sheet imaging was used to gain optical sectioning (*SI Appendix, Extended methods and Fig. S1*). Scale bar, 20  $\mu$ m. (B) Optical imaging of astrocyte water transport *in situ* in acute brain slices. Transmembrane water transport was triggered with hypo- and hypertonic solution, inducing water inflow and outflow that were respectively reflected by SRB fluorescence decrease and increase. Different durations of application of the hypo- or hypertonic solution caused water transport of different extents, translated by SRB fluorescence time courses of distinct amplitudes (n = 52 astrocytes, 4 mice). (C) Acutely blocking astrocyte AQP4 with TGN-020 caused intracellular water accumulation and swelling. *Left*, while no effect was seen under CTR condition (vehicle only, n = 23 astrocytes), TGN-020 (20  $\mu$ M) significantly decreased astrocyte SRB fluorescence (n = 30, 6 mice). Imaging was performed in acute brain slices of layer II/III S1 cortex. *Middle*, the downward slope was compared between the periods before and after the application of TGN-020. *Right*, illustration shows astrocyte aquaporin sustaining a tonic water efflux. Its blockade causes water accumulation and cell swelling. (D) *In vivo* validation of the effect of TGN-020 application on astrocyte water homeostasis. *Left*, fiber photometry was used for real-time recording of SRB fluorescence of astrocyte population in S1 cortex in freely moving mice, with saline (CTR) or TGN-020 being intraperitoneally injected when SRB was trapped in astrocytes. Fiber photometry recording shows that *in vivo* SRB injection resulted in rapid entry into mouse cortex and, in about one hour, led to astrocyte labeling (inset scale bar, 50  $\mu$ m). *Middle*, example response to saline and TGN-020. Relative to CTR, TGN caused a decrease in astrocyte SRB fluorescence and its oscillation range (n = 8 recordings per condition, 5 mice).

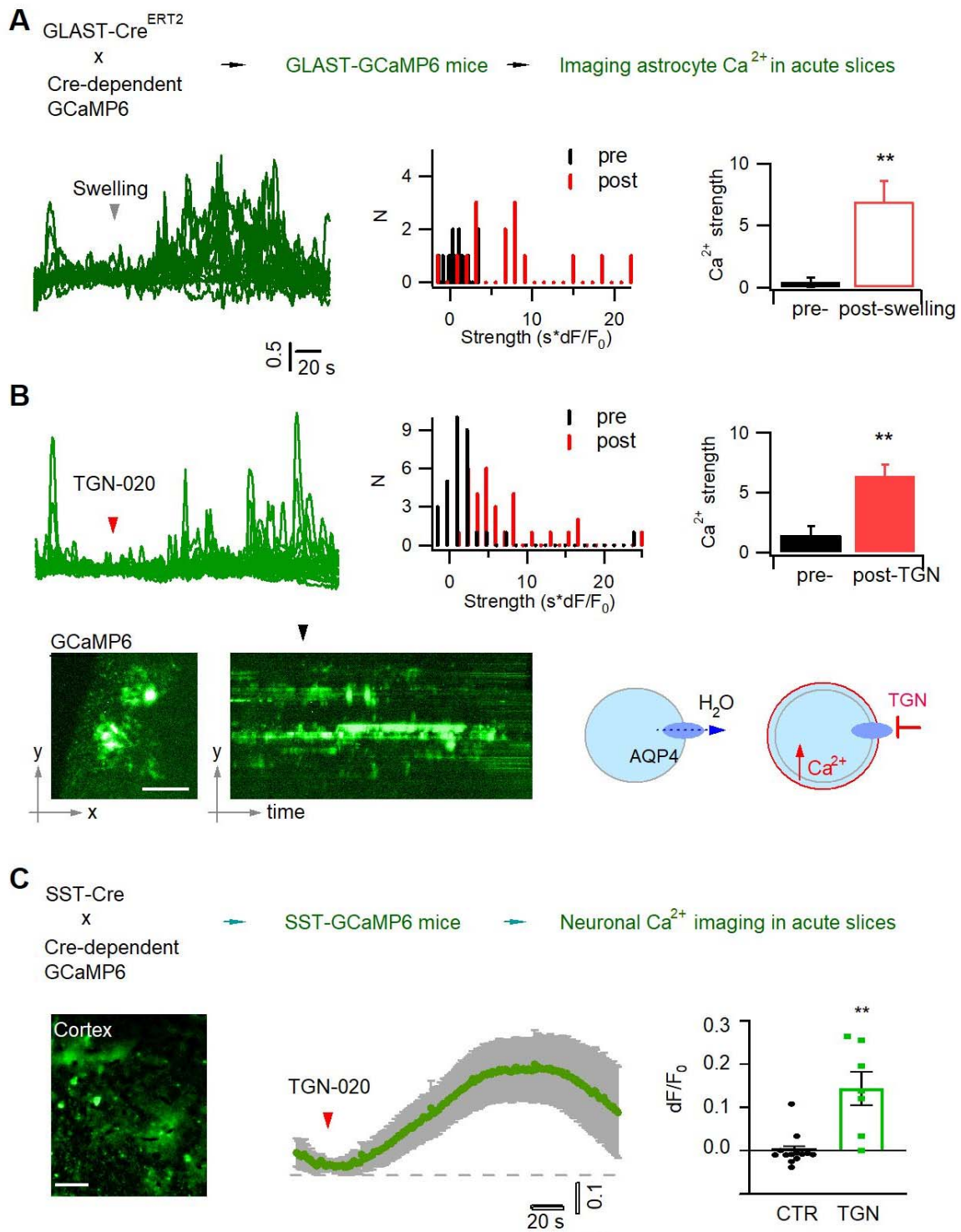


**FIGURE 2**



**Fig. 2.** Acutely blocking astrocyte aquaporin induces swelling-associated  $\text{Ca}^{2+}$  oscillation. (A) *In vivo* expression in astrocytes of the genetically encoded fluorescent  $\text{Ca}^{2+}$  indicator GCaMP6 for imaging astrocyte  $\text{Ca}^{2+}$  in acute brain slices. Light sheet microscopy was used to capture transient  $\text{Ca}^{2+}$  signals of local regions. As a positive control, astrocyte swelling was induced by hypotonic solution (100 mOsM) that caused  $\text{Ca}^{2+}$  changes from their homeostatic level. *Left*, representative time courses of swelling-induced  $\text{Ca}^{2+}$  changes in detected response regions; *middle to left*, the histogram distribution and bar representation showing the signal strengths that were derived from the temporal integral of individual  $\text{Ca}^{2+}$  time courses normalized per minute, before and after cell swelling (n = 15 astrocytes of three mice). (B) Astrocyte  $\text{Ca}^{2+}$  oscillation caused by acute aquaporin blocking with TGN-020 (n = 31 astrocytes of 5 mice), due to the inhibition of the tonic water efflux that led to astrocyte swelling as illustrated. Scale bar, 50  $\mu\text{m}$ . (C) Intercellular effect on SST interneurons of blocking astrocyte aquaporin water efflux. TGN-020 (20  $\mu\text{M}$ ) or the equal molar vehicle (CTR) was bath applied to acute cortical slices of SST-GCaMP6 mice (n = 7-12 measurements from 4 mice). Scale bar, 50  $\mu\text{m}$ .

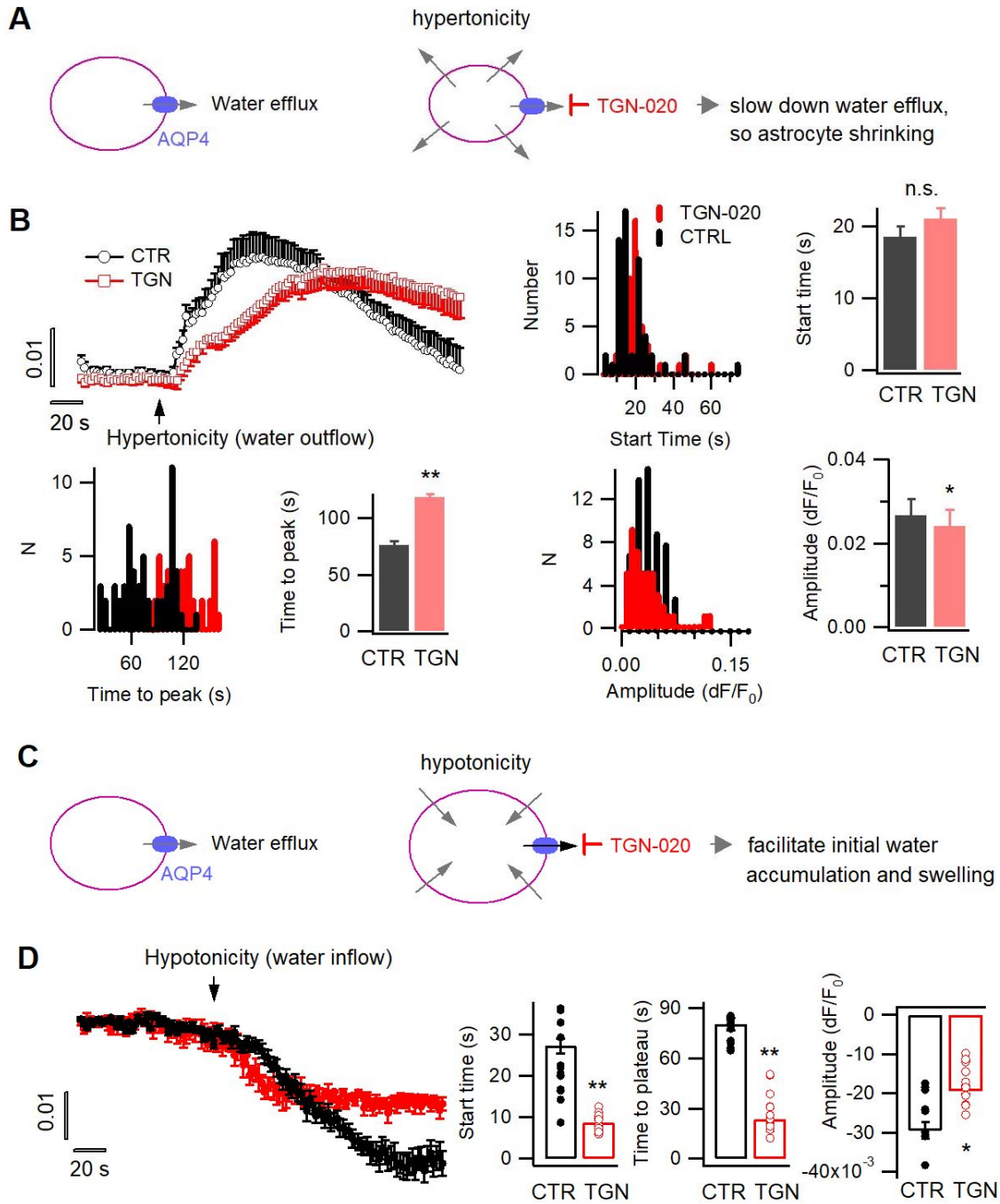


**FIGURE 3**

**Fig. 3.** Tonic water efflux via aquaporin modulates phasic transmembrane water transport and astrocyte volume response. (A) *Left*, in basal condition astrocyte aquaporin mediates a tonic water efflux. *Right*, protocol to induce water outflow from astrocytes, therefore their shrinking, by hypertonic extracellular solution (400 mOsM) in either control condition (CTR) or in the presence of AQP4 inhibitor TGN-020 (20  $\mu$ M). (B) Time courses of astrocyte SRB fluorescence increase upon the phasically induced water outflow, reflecting the occurrence of shrinking. The histograms and bar charts compare the start time, namely the delay between hypertonic solution application and rise in SRB fluorescence, the time to reach the peak of shrinking, and the absolute amplitude of water outflow-induced SRB increase (n = 58 astrocytes for CTR, and 47 astrocytes for TGN-020, four mice). (C) *Right*, protocol to trigger water inflow into astrocytes by hypotonic extracellular solution (100 mOsM) in either CTR solution or in the presence of TGN-020 (20  $\mu$ M). (D) Time courses of astrocyte SRB fluorescence decrease caused by water inflow, which also reflects concomitant cell swelling. In contrast to the observation with hypertonicity-induced water outflow and astrocyte shrinking, a reduction was observed for both the start time and the time-to-peak with TGN-020 (n = 12 astrocytes for CTR, and 12 astrocytes for TGN-020, four mice). TGN-020 led to a decrease in the absolute amplitude of astrocyte swelling.

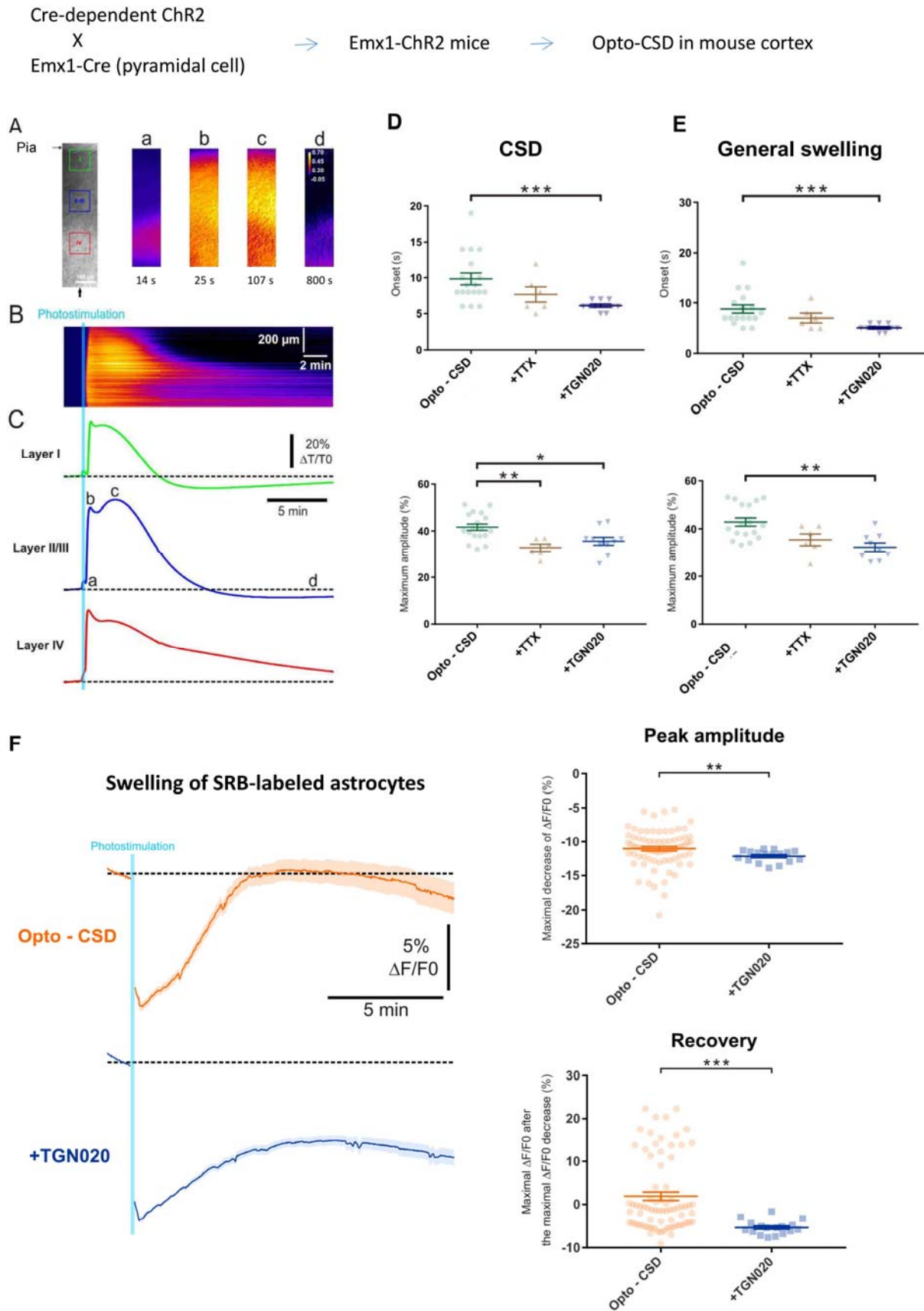


**FIGURE 4**

**Fig. 4.** AQP4-mediated tonic water outflow regulates global swelling in cortical parenchyma. CSD-associated general swelling was induced by photostimulating ChR2-expressing pyramidal cells in acute cortical slices, and recorded by imaging intrinsic optical signal (IOS) with infrared illumination. (A) Representative recording. The pia surface is on the upper side; green, blue and red squares correspond to regions of interest in Layers I, II-III and IV, respectively. Transmittance signals are represented in pseudocolor images at different time points post photostimulation. Scale bar, 100  $\mu\text{m}$ . (B) Kymograph showing the IOS changes in a radial line of interest indicated by a black arrow in A. The light blue line indicates the 10-s photostimulation that increases the infrared transmittance signal ( $dT/T_0$ ) across cortical layers, as also illustrated by the time courses; *a*, *b*, *c* and *d* correspond to the time points depicted in A. After the onset delay (*a*), the first (*b*) and second (*c*) peak of IOS are characteristic of the CSD and a prolonged general swelling, respectively. (D-E) TGN-020 (20  $\mu\text{M}$ ) inhibition of AQP4 reduced the initial onset and the maximal amplitude of both the CSD and general swelling ( $n = 6 - 18$  measurements from 13 mice per condition) in layer II/III cortex. Inhibiting spiking activity with TTX (1  $\mu\text{M}$ ) only affected the amplitude of the initial CSD response. (F) Astrocytes swelling, reflected by SRB fluorescence decrease, monitored in control condition ( $n = 75$  astrocytes) and in the presence of TGN-020 ( $n = 17$  astrocytes) in layer II/III cortex.

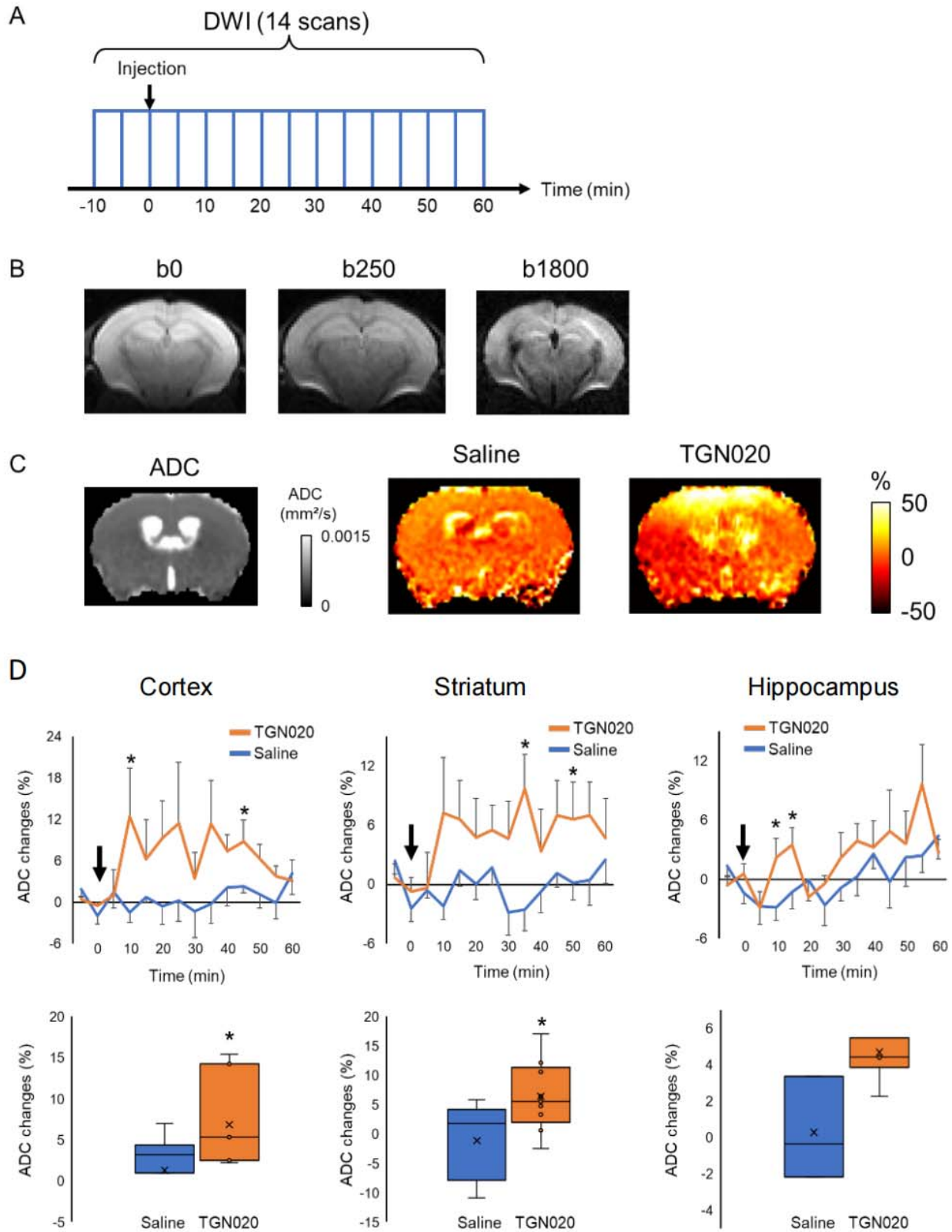


**FIGURE 5**

**Fig. 5.** Perturbing the tonic water efflux via astrocyte aquaporin alters brain water homeostasis. *In vivo* DW-MRI (7T) was employed to map water diffusion in the entire brain scale following the acute inhibition of astrocytic AQP4 (TGN-020, intraperitoneal injection, 200 mg/kg), with paralleled control experiments performed with saline injection. (A) Experimental protocol for DW-MRI. Saline or TGN020 was injected at 10 min after the start of acquisition. DWI was acquired every 5 min. (B) Representative image obtained at three different b values to derive the water diffusion rates. (C) *Left*, brain water diffusion rate was mapped by the calculation of apparent diffusion coefficient (ADC). *Right*, representative images illustrating the relative changes of ADC at 60 min after injection of saline or TGN-020. (D) Time courses depicting the temporal changes in ADC in the cortex, striatum, and hippocampus, revealing the regional heterogeneity. Arrowhead indicates the injection of saline or TGN-020 (n = 10 mice for saline injection, 9 mice for TGN-020).